

$J = 0$ nonmagnetic insulating state in K_2OsX_6 ($\text{X} = \text{F}, \text{Cl}$ and Br)

Yang Zhang,¹ Ling-Fang Lin,¹ Adriana Moreo,^{1,2} and Elbio Dagotto^{1,2}

¹*Department of Physics and Astronomy, University of Tennessee, Knoxville, TN 37996, USA*

²*Materials Science and Technology Division, Oak Ridge National Laboratory, Oak Ridge, TN 37831, USA*

(Dated: October 28, 2022)

In $4d/5d$ transition-metal systems, many interesting physical properties arise from the interplay of bandwidth, electronic correlations, and spin-orbit interactions. Here, using *ab initio* density functional theory, we systematically study the double-perovskite-like system K_2OsX_6 ($\text{X} = \text{F}, \text{Cl}$, and Br) with a $5d^4$ electronic configuration. Our main result is that the $J = 0$ nonmagnetic insulating state develops in this system, induced by strong spin-orbit coupling (SOC). Specifically, the well-separated OsX_6 octahedra lead to the cubic crystal-field limit and result in dramatically decreasing hoppings among nearest neighbor Os-Os sites. In this case, the three degenerate t_{2g} orbitals are reconstructed into two “effective” j_{eff} ($j_{\text{eff}} = 1/2$ and $j_{\text{eff}} = 3/2$ states) states separated by the strong SOC, opening a gap with four electrons occupying the $j_{\text{eff}} = 3/2$ orbitals. Furthermore, the hybridization between the Os $5d$ orbitals and the X ($\text{X} = \text{F}, \text{Cl}$, and Br) p orbitals increases from F to Br, leading the electrons in K_2OsF_6 to be more localized than in K_2OsCl_6 and K_2OsBr_6 , resulting in a smaller bandwidth for K_2OsF_6 than in the Cl- or Br-cases. Our results provide guidance to experimentalists and theorists working on this interesting family of osmium halides.

In the past decade, material systems with $4d$ or $5d$ transition-metal (TM) atoms, such as iridium and osmium, have attracted growing attention due to the exotic physical phenomena induced by the strong spin-orbit coupling (SOC) [1–5]. Compared to the nearly negligible SOC in $3d$ atoms, the strength of the SOC λ is substantially enhanced in those $4d/5d$ systems, leading to comparable values between λ , the hopping parameter t , the Hubbard repulsion U , and the Hund coupling J_H , resulting in several intriguing electronic phases arising from their competition, such as topological phases [6–9], the orbital-selective Peierls phase [10, 11], “spin-orbit Mott” insulating state [12, 13], Rashba-like splitting [14, 15], the anomalous Hall effect [16, 17], and quantum spin liquid ground states [18, 19].

In an octahedral d^4 system, under a cubic crystal-field condition, the five degenerate d orbitals split into two sets of bands (the higher e_g and lower t_{2g} bands) separated by a large crystal-field splitting energy Δ (~ 10 Dq) [20] [Fig. 1(a)]. Due to the competition among Δ , J_H and λ , many electronic states are possible for a d^4 system, such as $S = 2$, $S = 1$, and $J = 0$ states. For the $4d/5d$ system with d^4 configuration, such as Ru^{4+} , Os^{4+} , and Ir^{5+} , the four electrons will occupy the three degenerate t_{2g} orbitals, leading to a metallic state [Fig. 1(b)] because the t_{2g} orbitals are not fully occupied (four electrons in three t_{2g} orbitals). Then, by introducing the SOC effect, the three t_{2g} orbitals reconstruct into two “effective” j_{eff} ($j_{\text{eff}} = 1/2$ and $j_{\text{eff}} = 3/2$) states separated by the SOC [Fig. 1(a)]. Returning to the case $U = 0$, and considering the SOC with $\lambda > 0$, this system with a d^4 electronic configuration is expected to be a nonmagnetic (NM) insulator made of local two-hole $J = 0$ singlets [22, 23], where the band gap is opened by the strong SOC between the $j_{\text{eff}} = 1/2$ and $j_{\text{eff}} = 3/2$ states [Fig. 1(c)].

Recently, neutron scattering experiments revealed a

soft longitudinal magnon mode in Ca_2RuO_4 with the $4d^4$ configuration, which has been considered as a hallmark of a $J = 0$ singlet state quantum phase transition [24, 25]. In theory, this could lead to an exotic magnetically ordered state induced by the condensation of spin-orbit excitons [22, 23, 26–32]. Most searches for the $J = 0$ state have mainly focused on the $5d^4$ iridates systems. However, they display the $S = 1$ magnetic ground state or weak moments, instead of the NM insulator with the $J = 0$ singlets, such as the $5d^4$ iridates $\text{Ba}_3\text{YIr}_2\text{O}_9$ [33] and $\text{Ba}_3\text{ZnIr}_2\text{O}_9$ [34, 35]. Furthermore, the $J = 0$ state is still under debate for some double perovskite iridates with quite small noncubic crystal-field effect, such as Sr_2YIrO_6 [36, 37] and Ba_2YIrO_6 [38, 39]. Hence, the $J = 0$ state is still rare in real materials.

In general, the $4d/5d$ orbitals are much more spatially extended than the $3d$ orbitals, leading to an enhanced hopping t in the $4d/5d$ case, corresponding to a large bandwidth W in these systems (with the hopping t providing the scale). In this case, the large bandwidth W would induce the breakdown of the $J = 0$ singlet state [37, 40, 41], where an $S = 1$ state is obtained because $W \gg \lambda$. Furthermore, the $J = 0$ singlet ground state could also be suppressed by the large crystal-field splitting energy (between $d_{xz/yz}$ and d_{xy} orbitals) [40, 41], resulting in $S = 1$ or $S = 0$ states induced by Jahn-Teller distortion Q_3 [42]. Hence, a d^4 system with a strong SOC effect, small bandwidth W , and cubic crystal-field splitting becomes the best candidate to obtain the $J = 0$ NM singlet insulator.

K_2OsX_6 ($\text{X} = \text{F}, \text{Cl}$, and Br) has a double-perovskite-like structure, which is known to display the required conditions. This system has a $5d^4$ electronic configuration with strong SOC Os^{4+} ions, where the OsX_6 octahedra are at sufficiently large distance that they can be considered isolated from one another [Fig. 2]. K_2OsF_6 has the

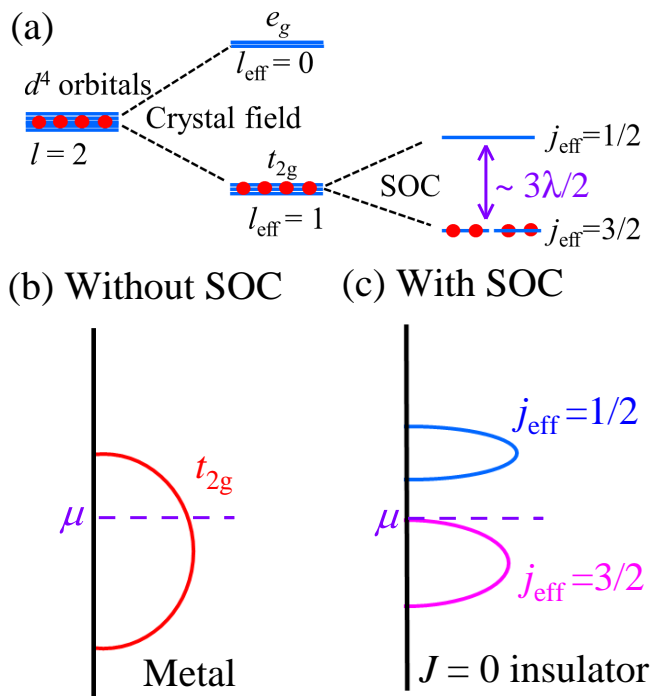


FIG. 1. (a) Schematic energy splitting of the d^4 electronic configuration with strong SOC under a cubic crystal field. Here, only the Hund rule is considered. Note the $j_{\text{eff}} = 3/2$ state has degeneracy four with $m = \pm 1/2$ and $m = \pm 3/2$. (b) The t_{2g} orbitals induce a metallic phase in a d^4 system without SOC and Hubbard U [21]. (c) Without Hubbard U , a $J = 0$ NM insulator is obtained in the d^4 system induced by SOC. Here, μ is the chemical potential.

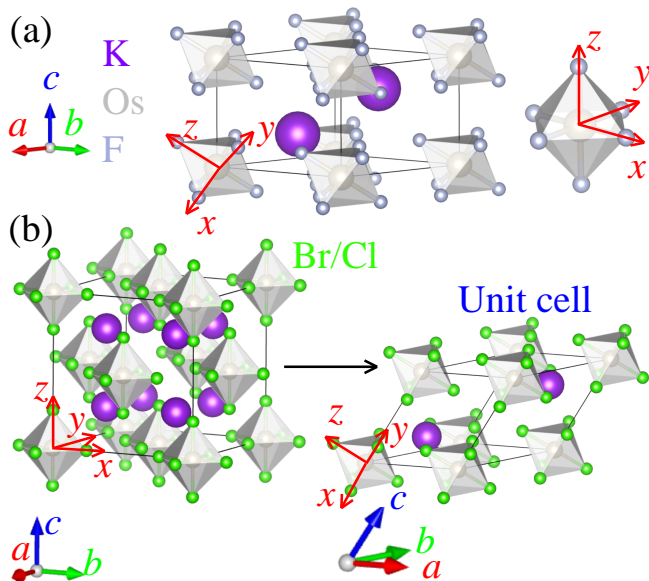


FIG. 2. Schematic crystal structure of K_2OsX_6 ($X = \text{F}, \text{Cl}$ and Br). (a) K_2OsF_6 with space group $P\bar{3}m1$ (No. 164). (b) K_2OsCl_6 and K_2OsBr_6 with space group $Fm\bar{3}m$ (No. 225). Crystal structures were visualized via the VESTA code [43].

space group $P\bar{3}m1$ (No. 164) while both K_2OsCl_6 and K_2OsBr_6 have the space group $Fm\bar{3}m$ (No. 225) [44]. In this family, due to the well-separated OsX_6 octahedra, the Jahn-Teller distortion is suppressed, leading to six equal Os-X bonds in this system, resulting in a nearly cubic crystal-field environment. In this case, the crystal-field splitting (between $d_{xz/yz}$ and d_{xy} orbitals) is suppressed. In addition, the hopping t between nearest-neighbor (NN) Os-Os sites should be small due to the Os-X-X-Os super-super exchange caused by the geometric structure of isolated OsX_6 octahedra. Hence, by considering the SOC in Os atoms, the $J = 0$ NM insulating state could possibly be stabilized in this family.

Based on the density functional theory (DFT) within the generalized gradient approximation (GGA) method and the Perdew-Burke-Ernzerhof revised for solids (PBEsol) exchange potential [45–49], we obtained that the relaxed crystal lattices are $a = b = 5.786$, and $c = 4.569$ Å for K_2OsF_6 , close to experimental values ($a = b = 5.777$ and $c = 4.544$ Å) [50]. We also found that the lattice constants of K_2OsCl_6 and K_2OsBr_6 ($a = b = c = 9.608$ Å for the Cl-case, and $a = b = c = 10.184$ Å for the Br-case) are in agreement with experiments ($a = b = c = 9.719$ Å for the Cl-case, and $a = b = c = 10.300$ Å for the Br-case) [51, 52]. To save computing resources, we used the unit cell structure of K_2OsCl_6 and K_2OsBr_6 [Fig. 2(b)] in the calculations below. In addition, we also calculated the phononic dispersion, finding that these structures are dynamically stable (see Fig. S1).

Next, we calculated the density of states (DOS) of K_2OsX_6 ($X = \text{F}, \text{Cl}$, and Br) in the NM state without SOC [42]. According to the DOS, the states near the Fermi level are mainly contributed by the $\text{Os-5d } t_{2g}$ orbitals, partially *hybridized* with $X-p$ orbitals, while most other X 's p states are located below the Os-5d energy states [Figs. 3(a-c)]. Note that the K's $4s$ states are located at high-energy bands (unoccupied states) while the K's $3p$ states occupy low-energy states below the X 's $3p$ states.

As shown in Figs. 3(a-c), the $X-p$ orbitals become closer to the Fermi level when X changes from F to Br. With increasing atomic radius from F to Br, the p components near the Fermi level become larger, leading to an increase in the $p-d$ hybridization tendency from F to Br. In this case, the Os's t_{2g} bands are more extended in K_2OsCl_6 ($W \sim 0.7$ eV) and K_2OsBr_6 ($W \sim 0.8$ eV) than in K_2OsF_6 ($W \sim 0.3$ eV), as shown in Figs. 3(a-c), suggesting stronger electronic correlations (U/W) in K_2OsF_6 . Furthermore, the energy splitting between the t_{2g} and e_g orbitals decreases from F (~ 3.3 eV) to Br (~ 2.6 eV) by estimating the weight-center positions of the energy bands. In addition, we also calculated the electron localization function (ELF) [53] for K_2OsF_6 , K_2OsCl_6 , and K_2OsBr_6 , respectively, as displayed in Fig. 3(d). The ELF picture indicates that the

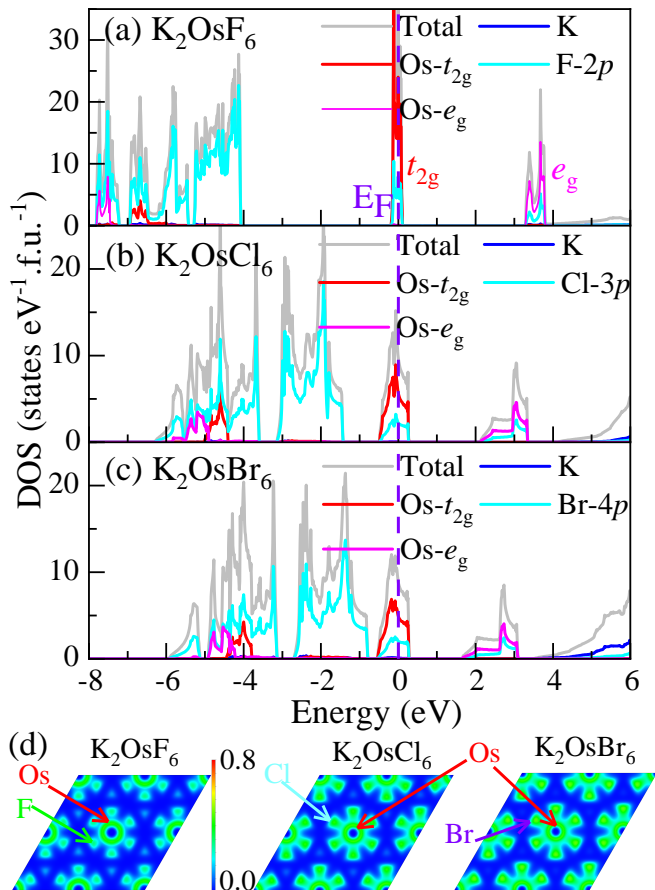


FIG. 3. (a)-(c) Projected density of states near the Fermi level based on the nonmagnetic states without SOC for (a) K_2OsF_6 , (b) K_2OsCl_6 and (c) K_2OsBr_6 , respectively. Gray: total; red: Os; blue: K; green: F; cyan: Cl; purple: Br. The Fermi level is marked by the vertical dashed magenta line. (a) Results for the $P\bar{3}m1$ (No. 164) structure of K_2OsF_6 . (b) Results for the $Fm\bar{3}m$ (No. 225) structure of K_2OsCl_6 . (c) Results for the $Fm\bar{3}m$ (No. 225) structure of K_2OsBr_6 . (d) Electron localization function for the a - b plane of nonmagnetic phases of K_2OsF_6 , K_2OsCl_6 , and K_2OsBr_6 respectively. Generally, $\text{ELF} = 0$ indicates no electron localization and $\text{ELF} = 1$ indicates full electron localization.

charges are more localized inside the Os-F bonds than the Os-Cl or Os-Br bonds, resulting in more hybridized p - d bonds in K_2OsF_6 than in K_2OsCl_6 or K_2OsBr_6 . For this reason, the bandwidth of K_2OsX_6 increases from F to Br, by considering the super-super exchange coupling (Os-X-X-Os) between two NN sites of Os. Furthermore, the stronger p - d hybridization tendencies would also reduce the SOC constants of Os atoms in the Cl- or Br-cases. This reduction was also experimentally observed in K_2IrX_6 ($X = \text{F}, \text{Cl}$ and Br) with the $5d^5$ configuration (572/444/420 meV for F/Cl/Br, respectively) [54].

To understand qualitatively the possible $J = 0$ state based on the maximally localized Wannier functions (MLWFs) method [55], we obtained the on-site energies

and hoppings for different Os's t_{2g} orbitals [56]. The spreads of t_{2g} orbitals of K_2OsF_6 are much smaller than that of K_2OsCl_6 and K_2OsBr_6 , indicating a more localized behavior in K_2OsF_6 than in the Cl- or Br- cases. Furthermore, the d_{xy} , d_{yz} , and d_{xz} orbitals have almost the same on-site energies, indicating that the crystal-splitting energy is nearly zero, thus achieving the condition needed for a stable $J = 0$ state. Moreover, the largest elements of the hopping matrix of NN Os-Os sites are 40, 88, and 95 meV for K_2OsF_6 , K_2OsCl_6 , and K_2OsBr_6 , respectively. Based on the values of hoppings, the on-site energies of the t_{2g} orbitals ($\Delta \sim 0$), using typical electronic correlations of Os atoms ($U \sim 1-2$ eV, $J_H \sim 0.3-0.4$ eV), and the strong SOC of the Os atom (~ 0.4 eV) [2, 5, 40, 41], the $J = 0$ NM state should be obtained, as discussed in Hubbard model studies [22, 23, 27]. In the limit of large on-site Hubbard coupling $U \gg \lambda$, naively the system would be an $S = 1$ Mott state where the electronic correlations play the dominant role. However, this is not the case we studied here. In addition, our GGA+ U +SOC calculations also provide a NM ground state for all F-, Cl- and Br-cases [42].

To better understand the possible $J = 0$ NM insulating state, we calculated the band structures with/without SOC or U for K_2OsF_6 , K_2OsCl_6 , and K_2OsBr_6 , respectively, as displayed in Fig. 4. First, let us focus on discussing the electronic structures for K_2OsF_6 . Without SOC and U effects, Fig. 4(a) displays a strong metallic behavior since the t_{2g} of Os states are not completely occupied (four electrons occupy three t_{2g} orbitals). By introducing the SOC effect, the t_{2g} orbitals of K_2OsF_6 are divided into $j_{\text{eff}} = 1/2$ and $j_{\text{eff}} = 3/2$ states, separated by an energy gap between the two j_{eff} states, as shown in Fig. 4(a). Then, four electrons of the Os^{4+} ($5d^4$ configuration) fully occupy the lower $j_{\text{eff}} = 3/2$ quadruplet, leading to an unoccupied $j_{\text{eff}} = 1/2$ doublet, resulting in a $J = 0$ NM insulator.

As shown in Fig. 4(b), we also studied the band structures with the electronic correlations included [57]. By only introducing the electronic correlation U , the band structure of the t_{2g} states of K_2OsF_6 is similar to the GGA case, where the t_{2g} bands of Os are not separated and keep metallic behavior. By considering both the SOC and U effects, the t_{2g} of K_2OsF_6 orbitals are reconstructed to the $j_{\text{eff}} = 1/2$ and $j_{\text{eff}} = 3/2$ states, opening a gap. In this case, the SOC plays the key role in deciding the nature of the insulating state, by separating the empty $j_{\text{eff}} = 1/2$ and fully-occupied $j_{\text{eff}} = 3/2$ states. The almost undistorted OsX_6 ($X = \text{F}, \text{Cl}$, and Br) octahedra are ideally separated, leading to a dramatic decrease in the hopping between Os-Os sites. In this quasi-disconnected geometry, the weak Os-X-X-Os superexchange interaction leads to the decreasing connectivity of the OsX_6 octahedra, resulting in a case close to the atomic limit. In the F-case, the large SOC effect achieves a $J = 0$ NM state by comparison with the small

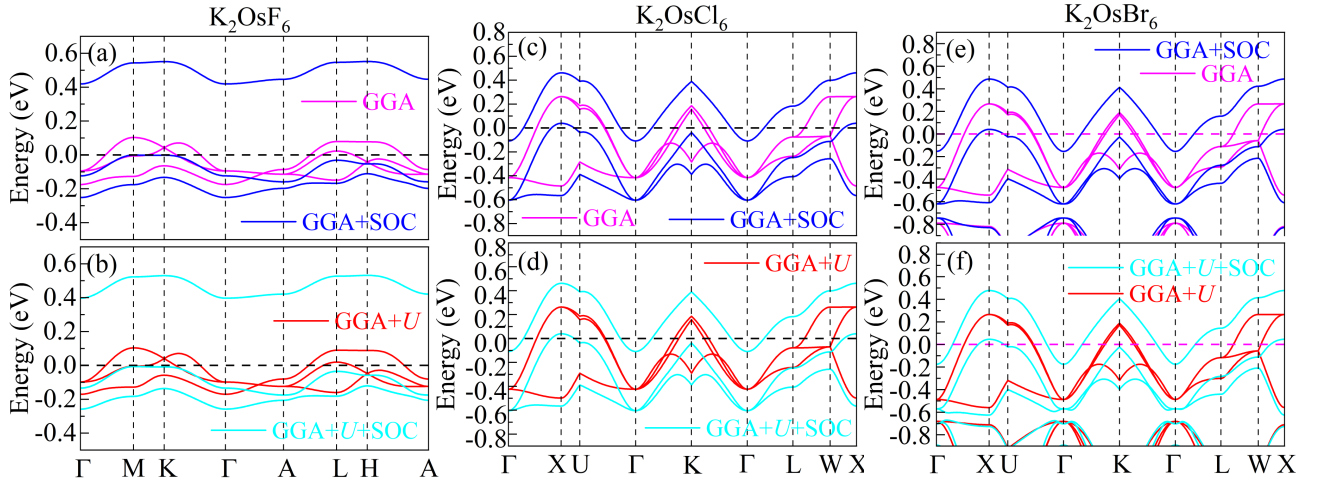


FIG. 4. Band structures of the NM state based on GGA, GGA+SOC, and GGA+ U +SOC for (a-b) K_2OsF_6 , (c-d) K_2OsCl_6 , and (e-f) K_2OsBr_6 , respectively. Here, the correlation effects were considered by the Liechtenstein formulation within the double-counting term [58], where the on-site Coulomb interaction used was $U = 2$ eV, and the Hund coupling was $J_H = 0.4$ eV for the Os atoms [59]. The Fermi level is the horizontal dashed line. (a-b) For K_2OsF_6 , the coordinates of the high-symmetry points in the Brillouin zone (BZ) are given by $\Gamma = (0, 0, 0)$, $M = (0.5, 0, 0)$, $K = (1/3, 1/3, 0)$, $A = (0, 0, 0.5)$, $L = (0.5, 0, 0.5)$ and $H = (1/3, 1/3, 0.5)$. (c-f) For K_2OsCl_6 or K_2OsBr_6 , the coordinates of the high-symmetry points in the BZ are given by $\Gamma = (0, 0, 0)$, $X = (0.5, 0, 0.5)$, $U = (0.625, 0.25, 0.625)$, $K = (0.375, 0.375, 0.75)$, $L = (0.5, 0.5, 0.5)$ and $W = (0.5, 0.25, 0.75)$.

hopping (~ 40 meV) and quenched crystal-field splitting.

Without SOC and U effects, the band structures of K_2OsCl_6 and K_2OsBr_6 show metallic behavior due to the partially occupied t_{2g} orbitals, as shown in Figs. 4(c) and (e). By introducing the SOC in K_2OsCl_6 and K_2OsBr_6 , the t_{2g} bands begin to separate and reconstruct into the $j_{\text{eff}} = 1/2$ and $j_{\text{eff}} = 3/2$ states [see Figs. 4(c) and (e)]. Different to the results for K_2OsF_6 , a band gap is not obtained with the SOC effect in both K_2OsCl_6 and K_2OsBr_6 , keeping a metallic state. Some Os $5d$ electrons partially occupy the $j_{\text{eff}} = 1/2$ states, contributing to the conductivity in both the Cl- and Br- cases. This can be understood intuitively. Due to the stronger $p-d$ hybridization tendencies in the Cl- or Br- cases than in the F- case, the bandwidth increases, and the SOC constants of Os atoms are reduced. Then, the hopping t could compete with the strong SOC λ , leading to a metallic phase with partially occupied $j_{\text{eff}} = 1/2$ states crossing the Fermi level. In this region, the $j_{\text{eff}} = 1/2$ and $j_{\text{eff}} = 3/2$ states are not totally separated. Then, if the strength of the SOC could continue to increase, the gap should finally open. Furthermore, similar to the results for K_2OsF_6 , the electronic correlation U would not separate the t_{2g} states and open a gap [Figs. 4(d) and (f)].

To better understand the SOC effect, we also calculated the band gaps within the GGA+SOC approximation by selecting various SOC strengths. As displayed in Fig. 5, the gap increases by enhancing the SOC strength [60]. Due to the small bandwidth of K_2OsF_6 , the gap can be opened by a small SOC strength ($\sim 50\%$). On the other hand, the insulating gap can be obtained

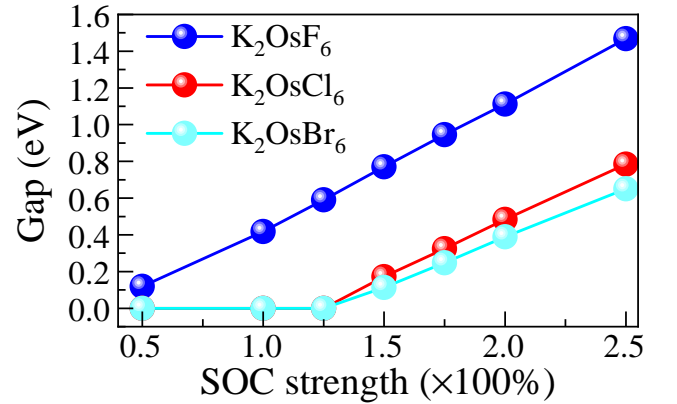


FIG. 5. Band gaps as a function of SOC strength for K_2OsF_6 , K_2OsCl_6 , and K_2OsBr_6 , respectively, within GGA+SOC calculations. Here, we do not introduce the Hubbard interaction U on Os sites because the SOC plays the key role to open the gap.

for a higher SOC strength ($\sim 150\%$) for K_2OsCl_6 and K_2OsBr_6 because the larger bandwidths of the Cl- or Br- cases leads to a competition between hopping t and SOC λ . Because the energy gap between the Os's $j_{\text{eff}} = 1/2$ and $j_{\text{eff}} = 3/2$ states is about $3\lambda/2$, we can estimate the SOC values by calculating the changes in the value of this energy gap under very small modifications in the SOC strength. In addition, we also estimated that the SOC values are about 0.467, 0.405, and 0.367 eV for K_2OsF_6 , K_2OsCl_6 , and K_2OsBr_6 , respectively. This

reduced tendency of SOC values in K_2OsX_6 is quite similar to the case of the K_2IrX_6 system with d^5 configuration [54]. By comparing the induced hoppings from F to Cl, this could explain the metallic behavior in Cl- and Br- cases. By continuing increasing the strength of the SOC, the gaps increase in K_2OsCl_6 and K_2OsBr_6 , as expected. In the strong SOC condition, the entire K_2OsX_6 ($X = \text{F}, \text{Cl}, \text{and Br}$) family could be considered to be a potential $J = 0$ NM insulator. The insulating vs. metallic character of the correlated system under study is decided by several factors related to different parameters (primarily t , λ , J_H , and U). As described in the text, the $J = 0$ state can be stabilized in a d^4 system only in a special range of parameters, namely under severe limitations, at least according to our calculations. For a complete physical picture, it would be important to study how the $J = 0$ state evolves by varying those many different parameters. Such effort will demand considerable computational resources and discussion, and they should be based on model calculations, beyond the scope of our present manuscript.

For the spin-orbital-entangled $J = 0$ NM insulating compounds, the excitonic $J = 1$ triplet state displays interesting magnetic order caused by the condensation of mobile spin-orbit excitons [22, 23]. The ordered moment is dependent on the competition between exchange interactions and the energy gap caused by the SOC. Furthermore, some possible interesting features can be obtained near the quantum critical point (QCP) in the $J = 1$ excitonic state, such as a Higgs mode [24] and magnons [5]. Our results for the K_2OsX_6 ($X = \text{F}, \text{Cl}, \text{and Br}$) family provide a starting point for experimentalists and theorists to work on the $J_{\text{eff}} = 0$ state or the $J = 1$ triplet excitations on this $5d^4$ system, such as in inelastic neutron scattering (INS) or resonant inelastic x-ray scattering (RIXS) experiments. In fact, the K site could be replaced by other $1+$ ions [61], such as Rb^+ , Cs^+ and $(\text{NH}_4)^+$, where the same $J = 0$ physics should be obtained. Due to the “zero-dimensional” geometry structure, the K site may be replaced by $2+$ ions, leading to a d^5 configuration, where the spin-orbital Mott state could be obtained. Hence, our results clearly provide a potential candidate system for experimentalists and theorists to work on this K-system and related materials.

In summary, we presented a systematic study of the K_2OsX_6 ($X = \text{F}, \text{Cl}, \text{and Br}$) family with a $5d^4$ electronic configuration by using DFT first-principles calculations. Due to the isolated geometry of the well-separated OsX_6 octahedra, this system is close to the cubic crystal-field limit and results in dramatically decreasing hoppings for nearest-neighbor Os-Os sites, providing a fertile condition for obtaining the $J = 0$ NM insulator. By introducing the SOC, the three degenerate t_{2g} orbitals are split into two separated “effective” j_{eff} ($j_{\text{eff}} = 1/2$ and $j_{\text{eff}} = 3/2$ states) states. In K_2OsF_6 , due to the small bandwidth of the Os $5d$ orbitals (~ 0.3 eV), the SOC ef-

fect is sufficiently strong to open a gap. Hence, four electrons of the Os^{4+} ($5d^4$ configuration) fully occupy the lower $j_{\text{eff}} = 3/2$ quadruplet, leading to an unoccupied $j_{\text{eff}} = 1/2$ doublet, resulting in a $J = 0$ NM insulator.

Furthermore, the hybridization between the Os $5d$ orbitals and X ($X = \text{F}, \text{Cl}, \text{and Br}$) p orbitals increases from F to Br, leading the electrons in K_2OsCl_6 and K_2OsBr_6 to be less localized than in K_2OsF_6 , resulting in a larger bandwidth for the Cl- or Br- cases ($\sim 0.7/0.8$ eV for K_2OsCl_6 and K_2OsBr_6 , respectively) than in the F case. In these compounds, the SOC λ competes with the hopping t in K_2OsCl_6 and K_2OsBr_6 , and the combination is not enough to open a gap because some electrons would occupy the $j_{\text{eff}} = 1/2$ states. By increasing the SOC strength to $\sim 150\%$, the $j_{\text{eff}} = 1/2$ and $j_{\text{eff}} = 3/2$ states become totally separated, obtaining the $J = 0$ NM insulator in K_2OsCl_6 and K_2OsBr_6 . Hence, our results should encourage experimentalists and theorists to continue working on this interesting family of osmium halides to achieve the $J_{\text{eff}} = 0$ state, and also $J = 1$ triplet excitations and excitonic magnetism.

The work of Y.Z., L.-F.L., A.M. and E.D. is supported by the U.S. Department of Energy (DOE), Office of Science, Basic Energy Sciences (BES), Materials Sciences and Engineering Division.

-
- [1] W. Witczak-Krempa, G. Chen, Y. B. Kim, and L. Balents, *Annu. Rev. Condens. Matter Phys.* **5**, 57 (2014).
 - [2] J. G. Rau, E. K.-H. Lee, and H.-Y. Kee, *Annu. Rev. Condens. Matter Phys.* **7**, 195 (2016).
 - [3] G. Cao, and P. Schlottmann, *Rep. Prog. Phys.* **81**, 042502 (2018).
 - [4] D. I Khomskii and S. V. Streltsov, *Chem. Rev.* **121**, 2992 (2021).
 - [5] T. Takayama, J. Chaloupka, A. Smerald, G. Khaliullin, and H. Takagi, *J. Phys. Soc. Jpn.* **90**, 062001 (2021).
 - [6] D. Xiao, W. Zhu, Y. Ran, N. Nagaosa, and S. Okamoto, *Nat Commun.* **2**, 596 (2011).
 - [7] M. Z. Hasan and C. L. Kane, *Rev. Mod. Phys.* **82**, 3045 (2010).
 - [8] X. Wan, A. M. Turner, A. Vishwanath, and S. Y. Savrasov, *Phys. Rev. B* **83**, 205101 (2011).
 - [9] B. Yan, and C. Felser, *Annu. Rev. Condens. Matter Phys.* **8**, 337 (2017).
 - [10] S. V. Streltsov and D. I. Khomskii, *Phys. Rev. B* **89**, 161112(R) (2014).
 - [11] Y. Zhang, L. F. Lin, A. Moreo, and E. Dagotto, *Phys. Rev. B* **104**, L060102 (2021).
 - [12] B. J. Kim, Hosub Jin, S. J. Moon, J.-Y. Kim, B.-G. Park, C. S. Leem, J. Yu, T. W. Noh, C. Kim, S.-J. Oh, J.-H. Park, V. Durairaj, G. Cao, and E. Rotenberg, *Phys. Rev. Lett.* **101**, 076402 (2008).
 - [13] Y. Zhang, L. F. Lin, A. Moreo, and E. Dagotto, *Phys. Rev. B* **105**, 085107 (2022).
 - [14] E. Bruyer, D. Di Sante, P. Barone, A. Stroppa, M.-H. Whangbo, and S. Picozzi, *Phys. Rev. B* **94**, 195402 (2016).

- [15] Y. Zhang, L. F. Lin, A. Moreo, S. Dong, and E. Dagotto, *Phys. Rev. B* **101**, 174106 (2020).
- [16] N. Mohanta, E. Dagotto, and S. Okamoto, *Phys. Rev. B* **100**, 064429 (2019).
- [17] M.-W. Yoo, J. Tornos, A. Sander, L.-F. Lin, N. Mohanta, A. Peralta, D. Sanchez-Manzano, F. Gallego, D. Haskel, J. W. Freeland, D. J. Keavney, Y. Choi, J. Stremper, X. Wang, M. Cabero, H. B. Vasili, M. Valvidares, G. Sanchez-Santolino, J. M. Gonzalez-Calbet, A. Rivera, C. Leon, S. Rosenkranz, M. Bibes, A. Barthelemy, A. Anane, E. Dagotto, S. Okamoto, S. G. E. te Velthuis, J. Santamaria, and J. E. Villegas, *Nat Commun.* **12**, 3283 (2021).
- [18] A. Kitaev, *Annals of Physics* **321**, 2 (2006).
- [19] H. Takagi, T. Takayama, G. Jackeli, G. Khaliullin, and S. E. Nagler, *Nat. Rev. Phys.* **1**, 264 (2019).
- [20] Dq means deci(ten) quanta of energy, where $10Dq$ represents the empirical octahedral crystal field splitting energy.
- [21] In the large U limit, the system (four electrons in three orbitals) should be a Mott insulator, where the gap is opened by the Hubbard U . However, the real system could be metallic or insulating depending on the competition of bandwidth W (corresponding to hopping t scale) and Hubbard interaction U . For example, see L. F. Lin, Y. Zhang, G. Alvarez, A. Moreo, and E. Dagotto, *Phys. Rev. Lett.* **127**, 077204 (2021).
- [22] G. Khaliullin, *Phys. Rev. Lett.* **111**, 197201 (2013).
- [23] O. N. Meetei, W. S. Cole, M. Randeria, and N. Trivedi, *Phys. Rev. B* **91**, 054412 (2015).
- [24] A. Jain, M. Krautloher, J. Porras, G. H. Ryu, D. P. Chen, D. L. Abernathy, J. T. Park, A. Ivanov, J. Chaloupka, G. Khaliullin, B. Keimer, and B. J. Kim, *Nat. Phys.* **13**, 633 (2017).
- [25] S.-M. Souliou, J. Chaloupka, G. Khaliullin, G. Ryu, A. Jain, B. J. Kim, M. Le Tacon, and B. Keimer, *Phys. Rev. Lett.* **119**, 067201 (2017).
- [26] C. Svoboda, M. Randeria, and N. Trivedi, *Phys. Rev. B* **95**, 014409 (2017).
- [27] N. Kaushal, J. Herbrych, A. Nocera, G. Alvarez, A. Moreo, F. A. Reboredo and E. Dagotto, *Phys. Rev. B* **96**, 155111 (2017).
- [28] A. J. Kim, H. O. Jeschke, P. Werner, and R. Valentí, *Phys. Rev. Lett.* **118**, 086401 (2017).
- [29] T. Sato, T. Shirakawa, and S. Yunoki, *Phys. Rev. B* **99**, 075117 (2019).
- [30] N. Kaushal, R. Soni, A. Nocera, G. Alvarez, and E. Dagotto, *Phys. Rev. B* **101**, 245147 (2020).
- [31] N. Kaushal, J. Herbrych, G. Alvarez, and E. Dagotto, *Phys. Rev. B* **104**, 235135 (2021).
- [32] P. Strobel, F. Aust, and M. Daghofer, *Phys. Rev. B* **104**, 115148 (2021).
- [33] T. Dey, A. V. Mahajan, R. Kumar, B. Koteswararao, F. C. Chou, A. A. Omrani, and H. M. Ronnow, *Phys. Rev. B* **88**, 134425 (2013).
- [34] A. Nag, S. Middey, Sayantika Bhowal, S. K. Panda, R. Mathieu, J. C. Orain, F. Bert, P. Mendels, P. G. Freeman, M. Mansson, H. M. Ronnow, M. Telling, P. K. Biswas, D. Sheptyakov, S. D. Kaushik, V. Siruguri, C. Meneghini, D. D. Sarma, I. Dasgupta, and S. Ray, *Phys. Rev. Lett.* **116**, 097205 (2016).
- [35] A. Nag, S. Bhowal, M. M. Sala, A. Efimenko, I. Dasgupta, and S. Ray, *Phys. Rev. Lett.* **123**, 017201 (2019).
- [36] G. Cao, T. F. Qi, L. Li, J. Terzic, S. J. Yuan, L. E. DeLong, G. Murthy, and R. K. Kaul, *Phys. Rev. Lett.* **112**, 056402 (2014).
- [37] S. Bhowal, S. Baidya, I. Dasgupta, and T. Saha-Dasgupta, *Phys. Rev. B* **92**, 121113(R) (2015).
- [38] J. Terzic, H. Zheng, F. Ye, H. D. Zhao, P. Schlottmann, L. E. De Long, S. J. Yuan, and G. Cao, *Phys. Rev. B* **96**, 064436 (2017).
- [39] S. Fuchs, T. Dey, G. Aslan-Cansever, A. Maljuk, S. Wurmehl, B. Büchner, and V. Kataev, *Phys. Rev. Lett.* **120**, 237204 (2018).
- [40] Y. Zhang, L. F. Lin, A. Moreo, and E. Dagotto, *Appl. Phys. Lett.* **120**, 023101 (2022).
- [41] Y. Zhang, L. F. Lin, A. Moreo, T. A. Maier, G. Alvarez, and E. Dagotto, *Phys. Rev. B* **105**, 174410 (2022).
- [42] See Supplemental Material at <http://link.aps.org/supplemental/xxxxxx> for Method details and more results, related to Refs. [21–23, 27, 43, 45–52, 55, 58, 62–64].
- [43] K. Momma and F. Izumi, *J. Appl. Crystallogr.* **44**, 1272 (2011).
- [44] K_2OsF_6 has a trigonal space group (No. 164), where the OsF_6 octahedra have a slightly distorted octahedron-like behavior, resulting in the angle of the F-Os-F bond not being strictly 90° . In K_2OsCl_6 and K_2OBr_6 , the OsF_6 or $OsBr_6$ octahedra are ideal without any distortion, leading to the ideal 90° bonds in the cubic structure (No. 225).
- [45] G. Kresse and J. Hafner, *Phys. Rev. B* **47**, 558 (1993).
- [46] G. Kresse and J. Furthmüller, *Phys. Rev. B* **54**, 11169 (1996).
- [47] P. E. Blöchl, *Phys. Rev. B* **50**, 17953 (1994).
- [48] J. P. Perdew, K. Burke, and M. Ernzerhof, *Phys. Rev. Lett.* **77**, 3865 (1996).
- [49] J. P. Perdew and A. Ruzsinszky, and G. I. Csonka and O. A. Vydrov and G. E. Scuseria and L. A. Constantin and X. Zhou and K. Burke, *Phys. Rev. Lett.* **100**, 136406 (2008).
- [50] S. I. Ivlev, A. V. Malin, A. J. Karttunen, R. V. Ostvald, and F. Kraus, *J. Fluorine Chem.* **218**, 11 (2019).
- [51] H. Takazawa, S. Ohba, Y. Saito and M. Sano, *Acta Cryst. B* **46**, 166 (1990).
- [52] J. D. McCullough, *Z Kristallogr - Cryst Mater.* **94**, 143 (1936).
- [53] A. Savin, O. Jepsen, J. Flad, O.-K. Andersen, H. Preuss, and H. G. von Schnering, *Angew. Chem. Int. Ed.* **32**, 187 (1992).
- [54] D. Reig-i-Plessis, T. A. Johnson, K. Lu, Q. Chen, J. P. C. Ruff, M. H. Upton, T. J. Williams, S. Calder, H. D. Zhou, J. P. Clancy, A. A. Aczel, and G. J. MacDougall, *Phys. Rev. Mater.* **4**, 124407 (2020).
- [55] A. A. Mostofi, J. R. Yates, Y. S. Lee, I. Souza, D. Vanderbilt, and N. Marzari, *Comput. Phys. Commun.* **178**, 685 (2007).
- [56] Here, we constructed three disentangled Wannier functions based on the MLWFs method [55] to fit the low-energy DFT bands near the Fermi level, involving the t_{2g} orbital basis (d_{xy} , d_{yz} , and d_{xz}) for each Os atom in the nonmagnetic phase without SOC. The local basis is marked in the inset of Fig. 1, with the x -, y -, or z -axis along with the Os- X directions. As shown in Fig. S2, the DFT bands near the Fermi level are fitted very well with the Wannier bands obtained from MLWFs. Due to a slightly distorted octahedron-like behavior in K_2OF_6 , the calculated on-site energies of t_{2g} orbitals are slightly different (~ 0.6) meV, approaching the cubic filled con-

- dition. Due to the undistorted octahedra in K_2OCl_6 and K_2OBr_6 , we obtained the same on-site energy for the three degenerate t_{2g} orbitals.
- [57] The values $U = 2$ and $J = 0.4$ eV may be slightly larger for the Os site, especially for F-case. For example, cRPA calculation indicates that the U of the Os site is smaller than 1 eV, see B. Kim, P. Liu, Z. Ergönenc, A. Toschi, S. Khmelevskiy, and C. Franchini, *Phys. Rev. B* **94**, 241113(R) (2016). However, in our case of the $J = 0$ state, the SOC plays the key role to open the gap, not U .
- [58] A. I. Liechtenstein, V. I. Anisimov, and J. Zaanen, *Phys. Rev. B* **52**, R5467 (1995).
- [59] Note that the ratio $J_H/U = 0.20$ is similar to the value 0.25 widely used in iron superconductors. See for example Q. Luo, G. Martins, D.-X. Yao, M. Daghofer, R. Yu, A. Moreo, and E. Dagotto, *Phys. Rev. B* **82**, 104508 (2010). Furthermore, we also tested different J_H and U values and the conclusions do not change [see Figs. S4-S6].
- [60] Here, 100% SOC means the standard SOC calculations in the original DFT code. Then, we change different strength ratios for the SOC to study the electronic structures based on GGA+SOC calculations, i.e. 200% indicates two times of original SOC strength.
- [61] R. L. Armstrong, *Phys. Rep.* **57**, 343 (1980).
- [62] L. Chaput, A. Togo, I. Tanaka, and G. Hug, *Phys. Rev. B* **84**, 094302 (2011).
- [63] A. Togo, I. Tanaka, *Scr. Mater.* **108**, 1 (2015).
- [64] Y. Zhang, L.-F. Lin, G. Alvarez, A. Moreo, and E. Dagotto, *Phys. Rev. B* **104**, 125122 (2021).